Synthesis, Characterisation and Structure Determination of 3-[(1Z)-{2-[bis({[(2-methylphenyl)methyl]sulfanyl})methylidene]hydrazin-1-ylidene}methyl]benzene-1,2-diol

Enis Nadia Md Yusof [a,b], Edward R.T. Tiekink[c *], Mukesh M. Jotani[d], Michela I. Simone[b,e], Alister J. Page[b] , Thahira B.S.A. Ravoof[a] *

[a] *Department of Chemistry, Faculty of Science, Universiti Putra Malaysia, 43400 UPM Serdang, Selangor, Malaysia*

[b] *Discipline of Chemistry, School of Environmental and Life Sciences, University of Newcastle, University Drive, Callaghan, NSW 2308, Australia.*

[c] *Research Centre for Crystalline Materials, School of Science and Technology, Sunway University, 47500 Bandar Sunway, Selangor Darul Ehsan, Malaysia.*

[d] *Department of Physics, Bhavan's Sheth R. A. College of Science, Ahmedabad, Gujarat 380001, India.*

[e] *Priority Research Centre for Chemical Biology & Clinical Pharmacology, University of Newcastle, University Drive, Callaghan, NSW 2308, Australia.*

Abstract A light-yellow crystalline product (**1**), which was isolated after one week from the filtrate of the reaction between S-2-methylbenzyldithiocarbazate and 2,3-dihydroxybenzaldehyde, was characterised by single crystal X-ray diffraction, FTIR and NMR spectroscopic analyses. The experimental molecular structure of **1** has been established by X-ray crystallography and showed, to a first approximation, a planar $C_2N_2S_2$ + dihydroxyphenyl region that has an almost orthogonal relationship to the rings of the pendant S-bound benzyl groups. This structure has been verified via density functional theory calculations using the B3LYP/6311G(d,p) level of theory. The molecular packing featured linear supramolecular chains along the b-axis sustained by tolyl-C–H…N(imine) and tolyl-C–H…π(tolyl) interactions; the importance of these contacts is indicated by a Hirshfeld surface analysis.

Keywords dithiocarbazate diester; single crystal X-ray diffraction analyses; DFT; 2,3-dihydroxybenzaldehyde

1. Introduction

Dithiocarbazates are hard-soft nitrogen-sulphur donor ligands. Since the 1980's, many Schiff bases derived from dithiocarbazates have been synthesised, characterised and investigated especially for their pharmaceutical potential [1]. The variety of coordination modes in dithiocarbazates and the ease of modification by introducing different organic substituents to the dithiocarbazate derivatives [2–7] have been of interest as relatively small modifications in the structural backbone often gives rise to major differences in their biological properties. For example, many of these compounds display selective in vitro biological activity against several cancer cell lines [4,5,7–11]. In addition, some dithiocarbazate ligands and their metal complexes have also investigated for other applications including as nonlinear optical (NLO) materials with diverse magnetic and electrochemical properties [12–14].

The single-crystal X-ray diffraction analysis of S-benzyldithiocarbazate (SBDTC) was reported thirty years after its synthetic procedure was first established [15] and since then much work has been carried out on the synthesis of analogous S-substituted dithiocarbazates: S-allyl [16], isomeric S-2-/3-/4-picolyl [17,18], isomeric S-2-/3-/4-methylbenzyl [7,19,20], S-napthylmethyl [21], S-quinolin-2yl-methyl [21], S-4-nitrobenzyl [5] and S-4-chlorobenzyl [22] dithiocarbazates and their transition metal complexes.

As part of our on-going study on Schiff bases derived from S-2-methylbenzyldithiocarbazate (S2MBDTC) [7] and 2,3-dihydroxybenzaldehyde, we report herein the unexpected formation of a compound that crystallised during the routine synthetic procedure of S-2-methylbenzyl-β-N-(2,3-dihydroxybenzylmethylene)dithiocarbazate. The product, 3-[(1Z)-{2-[bis({[(2-methylphenyl)methyl]sulfanyl})methylidene]hydrazin-1-ylidene}methyl]benzene-1,2-diol (**1**), formed from the filtrate after it was left standing for one week, which was fully characterised by X-ray crystallography, NMR, FT-IR and UV/Vis spectroscopy. To further support the experimental data, density functional theory (DFT) calculations have been used to analyse the structural and spectroscopic characteristics of this compound.

2. Experimental Section

2.1. Instrumentation

Melting points were measured using an Electrothermal digital melting point apparatus. FT-IR spectra were recorded using a PerkinElmer Spectrum 100 with Universal ATR Polarization in the 4000–280 cm^{-1} range. ^{1}H- and ^{13}C-NMR spectra were recorded using an NMR JNM

ECA400 spectrometer with tetramethylsilane (TMS) as the internal reference (placed at 0 ppm). Electronic spectra were recorded in DMSO on a Shimadzu UV-2501 PC recording spectrophotometer (1000–200 nm).

2.2. Materials

All chemicals and solvents were of analytical grade and were used without further purification. Chemicals: 2-methylbenzyl chloride (ACROS), potassium hydroxide (HmbG), hydrazine hydrate (Fluka), carbon disulphide (Merck) and 2,3-dihydroxybenzaldehyde (Merck) Solvents: acetonitrile (Fisher), absolute ethanol (QRec), ethanol (QRec) and methanol (Systerm).

*2.3. Synthesis of S2MBDTC and the formation of 3-[(1Z)-{2-[bis({[(2-methylphenyl)methyl]sulfanyl})methylidene]hydrazin-1-ylidene}methyl] benzene-1,2-diol (**1**)*

S-2-methylbenzyldithiocarbazate (S2MBDTC) was synthesised according to a previously reported method [7]. S2MBDTC (2.12 g) was dissolved in 100 ml acetonitrile/ethanol (9:1) solution with an equimolar quantity of 2,3-dihydroxybenzaldehyde added to it. The mixture was stirred and heated (~80°C) for 2 h. The resultant mixture then was allowed to cool to room temperature and the expected product, S-2-methylbenzyl-β-N-(2,3-dihydroxybenzylmethylene)dithiocarbazate that formed was filtered. The filtrate was kept at room temperature. Light-yellow crystals formed after a period of one week which were analysed by single crystal X-ray diffraction analysis and were found to be an unexpected product, 3-[(1Z)-{2-[bis({[(2-methylphenyl)methyl]sulfanyl})methylidene]hydrazin-1-ylidene}methyl]benzene-1,2-diol (**1**). The synthetic scheme for the formation of **1** is shown in Scheme 1. M.p.: 153-155°C. FT-IR (ATR, cm^{-1}): 3542, 3497 *ν*(O-H); 1608, *ν*(C=N); 1257, *ν*(N-N); 978, *ν*(C-S). ^{1}H-NMR ($CDCl_3$) δ (ppm): 2.41, 2.46 (s, 2 x 3H, 2 x CH_3), 4.31, 4.51 (s, 2 x 2H, 2 x CH_2), 6.84-7.58 (m, 11H, Ar-H), 8.55 (s, 1H, CH) 11.11, 9.89 (s, 2 x 1H, 2 x OH); ^{13}C-NMR (DMSO-d_6) δ (ppm): 19.2, 19.3 (2 x CH_3), 34.0, 35.3 (2 x CH_2), 117.4, 117.5, 119.7, 122.9, 126.4, 126.4, 128.2, 128.3, 130.2, 130.5, 130.7, 130.7, 132.7, 133.3, 137.2. 137.3, 144.8, 146.3 (18 x aromatic-C), 159.9 (C=N), 167.3 (S-C-S). UV/Vis in DMSO, λ_{max} nm (log ε in L mol $^{-1}$$cm^{-1}$): 328 (4.48).

*2.4. Single crystal X-ray structure determination of **1***

Intensity data for light-yellow **1** were measured at T = 153 K on an Oxford Diffraction Gemini E CCD diffractometer fitted with Mo Kα radiation (λ = 0.71073 Å) so that θ_{max} was 29.4°. Data reduction, including analytical absorption correction, was accomplished with CrysAlisPro [23]. Of the 10166 measured reflections, 5026 were unique (R_{int} = 0.036) and of these, 3391 data satisfied the $I \geq 2\sigma(I)$ criterion of observability. The structure was solved by direct-methods [24] and refined (anisotropic displacement parameters, C-bound H atoms in the riding model approximation). A weighting scheme $w = 1/[\sigma^2(F_o^2) + 0.051P^2 + 0.384P]$ where $P = (F_o^2 + 2F_c^2)/3)$ on F^2 [25] was introduced. Based on the refinement of 279 parameters, the final values of R and wR (all data) were 0.053 and 0.130, respectively. The molecular structure diagram was generated with ORTEP for Windows [26] and the packing diagrams with DIAMOND [27]. Crystal data for $C_{24}H_{24}N_2O_2S_2$ (**1**): M = 436.60, monoclinic space group $P2_1/n$, a = 10.8207(5) Å, b = 9.0774(4) Å, c = 22.5231(10) Å, β = 98.090(4)°, V = 2190.29(17) Å^3, Z = 4, D_x = 1.324 g cm^{-3}, F(000) = 920, μ = 0.266 mm^{-1}. CCDC deposition number: 1816156.

2.5. Density Functional Theory Calculations

The gas-phase geometry of **1** in the electronic ground state was fully optimised using density functional theory (DFT). The hybrid B3LYP [28,29] exchange correlation functional was used in conjunction with a 6-311G(d,p) Pople basis set. The experimental X-ray crystallographic structure of **1** was used as the initial geometry. Harmonic vibrational frequencies were calculated to ensure that the optimized geometry represented the local minimum of the potential energy surface. The electronic excitations of **1** were computed using time-dependent density functional theory (TD-DFT) [30,31] and included solvation effects (DMSO) via the polarisable continuum method (PCM). The predicted ^{1}H and ^{13}C NMR chemical shifts in chloroform were obtained using the GIAO approach [32,33]. All computations were performed using the Gaussian09 (G09) program [34].

3. Results and Discussion

S-2-methylbenzyldithiocarbazate (S2MBDTC) is an ester produced from the reaction of hydrazine hydrate with carbon disulphide followed by the alkylation or arylation of the dithiocarbazate salts with different alkyl/aryl halides, at temperatures below 5°C and in the presence of a base (potassium hydroxide was used in this reaction) [5,7,16–22]. However, the

concentration of potassium hydroxide plays an important role in determining the formation of the esters, where sometimes diesters are formed as a secondary by-product [35]. This occurs via a second S_N2 reaction occurring through the thione sulphur atom reacting with a second molecule of 2-methylbenzylchloride at higher temperatures, followed by a second deprotonation of S2MBDTC. Similar diester formation have been reported by other researchers [36–38].

As shown in the reaction scheme (**Scheme 1**), the inseparable and unstable intermediate mixture of S2MBDTC and diester was reacted with 2,3-dihydroxybenzaldehyde in acetonitrile:ethanol (9:1) at 80°C for 2 hours which produced two light-yellow products that were chemically stable and separable: S2MdiOH Schiff base (desired product for biological work) and an unexpected product (**1**). In our synthetic protocol, the S2MdiOH Schiff base formed from the reaction solvent mixture immediately upon cooling and was collected via filtration, whilst product (**1**) - present in the filtrate - crystallised after one week at room temperature.

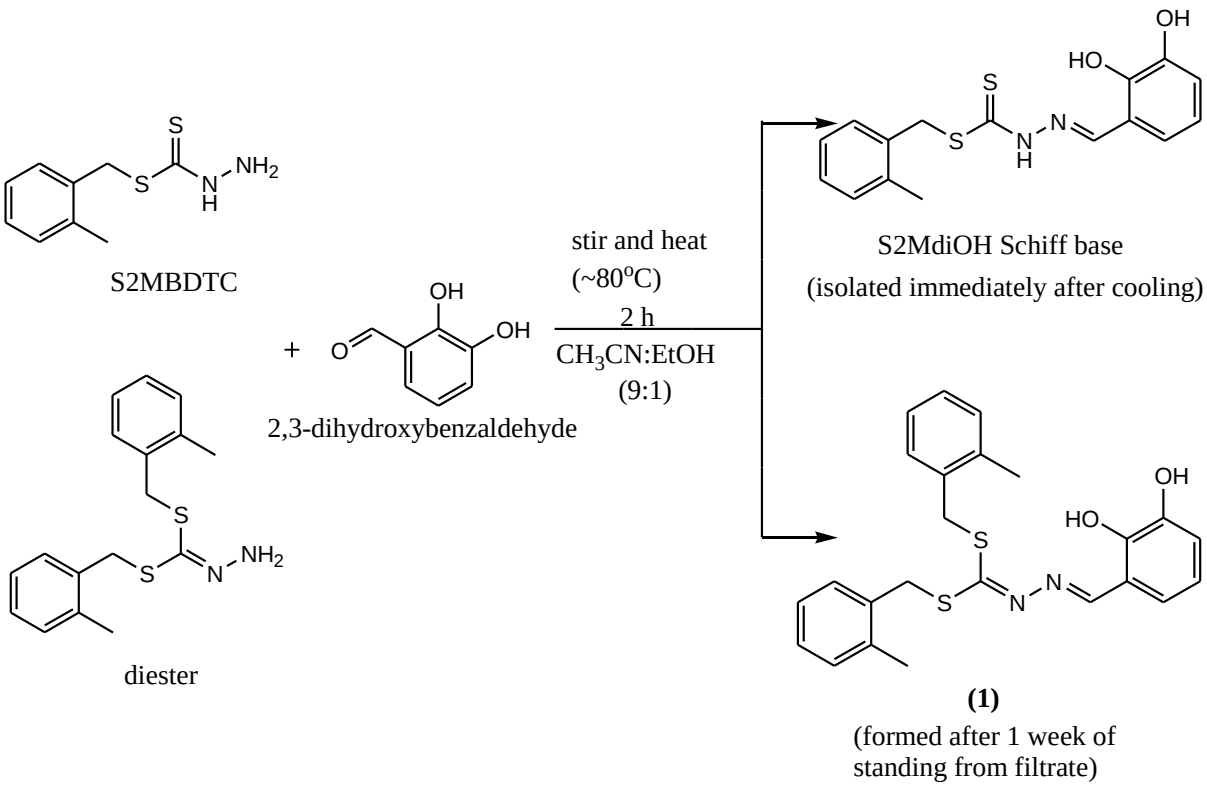

Scheme 1: Formation of **1**

The proposed mechanism leading to the formation of product **1** is shown in **Scheme 2**. **1** formed by nucleophilic addition via several steps: **(a)** nucleophilic attack of diester

dithiocarbazate onto the carbonyl C of the aldehyde (2,3-dihydroxybenzaldehyde), **(b) (c)** Bronsted-Lowry acid-base reactions, **(d)** dehydration reaction and **(e)** Bronsted-Lowry acid-base reaction. The spectroscopic studies and computational calculations were in agreement with the confirmed structure of the compound *via* crystallographic analysis.

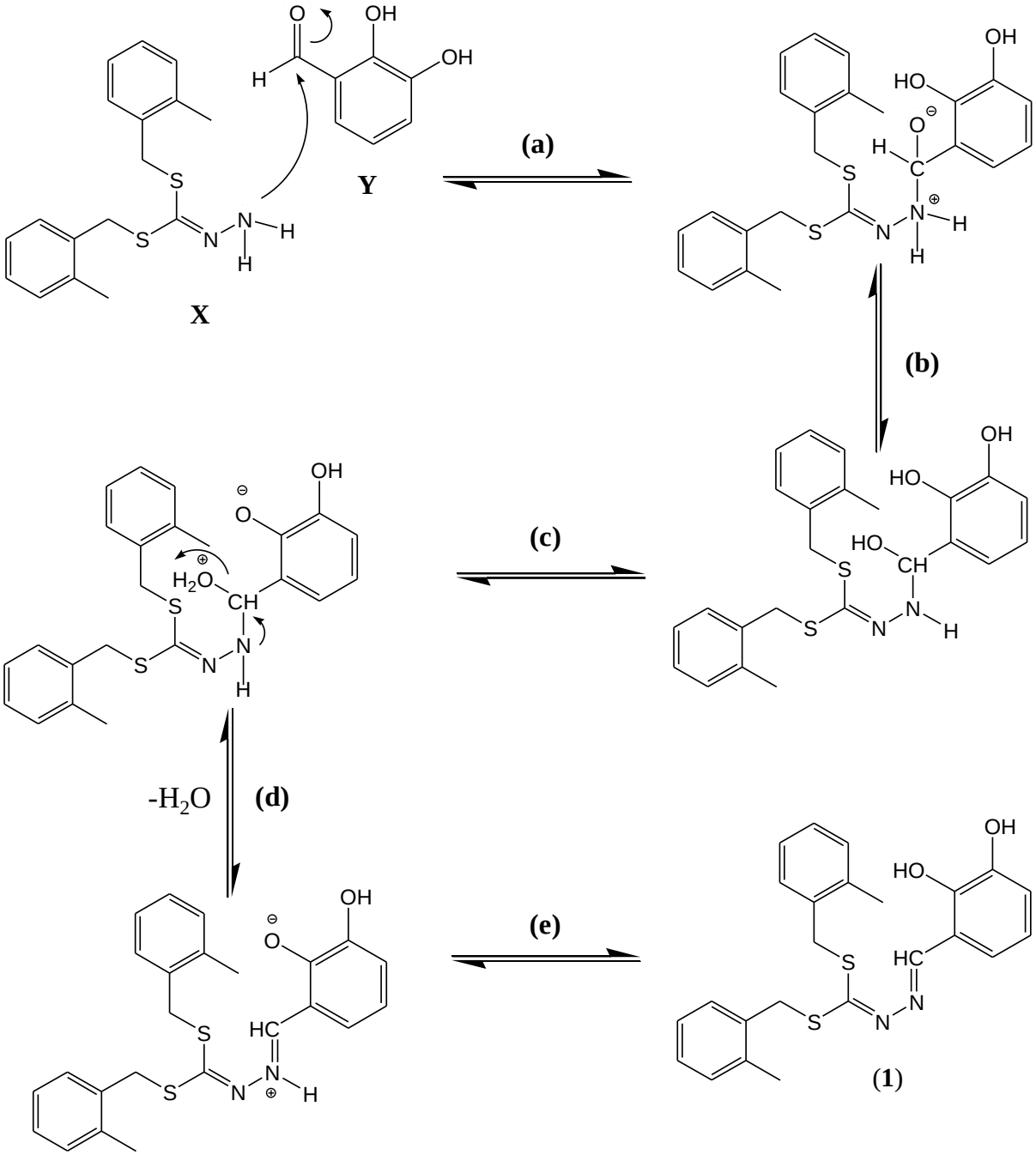

Scheme 2. Working hypothesis for the likely reaction mechanism for the formation of **1** from starting materials **X** (diester dithiocarbazate) and **Y** (2,3-dihydroxybenzaldehyde)

*3.1 Crystal and molecular structure of **1***

The molecular structure of **1** is illustrated in Fig. 1 and features a central and planar $C_2N_2S_2$ core with a r.m.s. deviation of the six fitted atoms of 0.0160 Å, and with maximum deviations above and below the plane of 0.0287(16) and 0.0238(12) Å for the N2 and C18 atoms, respectively. The dihydroxyphenyl ring was inclined to this plane forming a dihedral angle of 4.15 (11)°, reflecting a small twist about the hydrazine N1–N2 bond as seen in the value of the C1–N1–N2–C18 torsion angle of 177.0(2)°. By contrast, the substituted benzyl rings are almost orthogonal to the central plane forming dihedral angles of 71.57(5) and 84.01(5)° with the S1- and S2-bound groups, respectively. The benzyl rings were splayed out, forming a dihedral angle of 63.53(7)°. The molecule featured two intramolecular hydrogen bonds, namely hydroxyl-O–H…O(hydroxyl) and hydroxyl-O–H…N(imine); structural details are given in Table 1. A discussion of the key geometric parameters is presented along with those obtained from DFT analysis in Section 3.2.

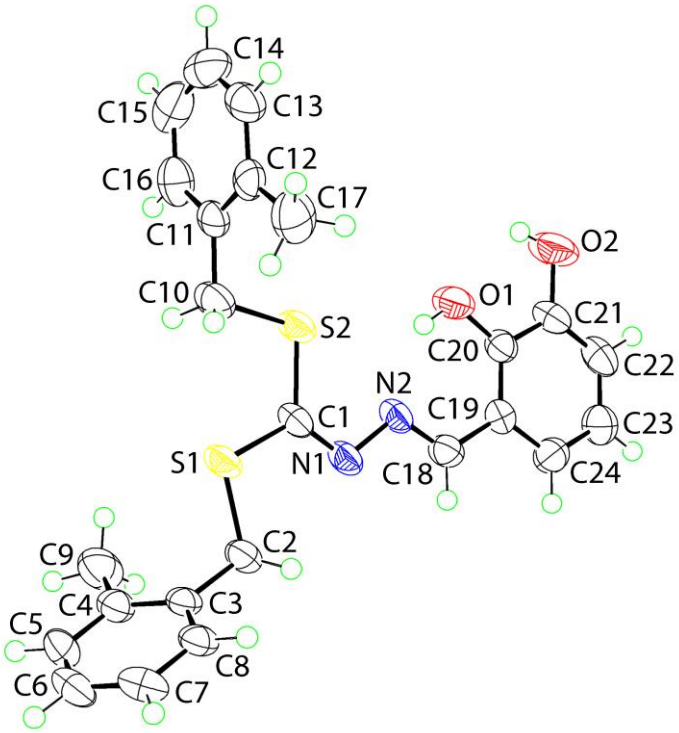

Fig. 1. ORTEP diagram of **1** showing atom labels and displacement ellipsoids at the 70% probability level.

Table 1

Geometric parameters (Å, °) characterising intra- and inter-molecular contacts in **1**.

A	H	B	H…B	A…B	A–H…B	Symmetry operation
O1	H1o	N2	1.901(18)	2.627(3)	144(2)	x, y, z
O2	H2o	O2	2.20(3)	2.680(3)	116(3)	x, y, z
C16	H16	N1	2.59	3.535(3)	172	1-x, 1-y, -z
C14	H14	Cg(C3-C8)	2.83	3.635(3)	144	1-x, -y, -z

Conventional hydrogen bonding interactions were absent in the molecular packing of **1** owing to the participation of the O1, O2 and N2 atoms in intramolecular interactions. Centrosymmetrically-related molecules were connected into dimeric aggregates via tolyl-C–H…N(imine) interactions, Table 1. The aggregates were connected into a linear supramolecular chain along the b-axis via tolyl-C–H…π(tolyl) interactions, Fig. 2a and Table 1. Chains pack without directional interactions between them according to the distance criteria assumed in PLATON [39]. A view of the unit cell contents is shown in Fig. 2b. A more detailed analysis of the supramolecular association in the crystal of **1** is given in the discussion of the Hirshfeld surfaces in Section 3.2.

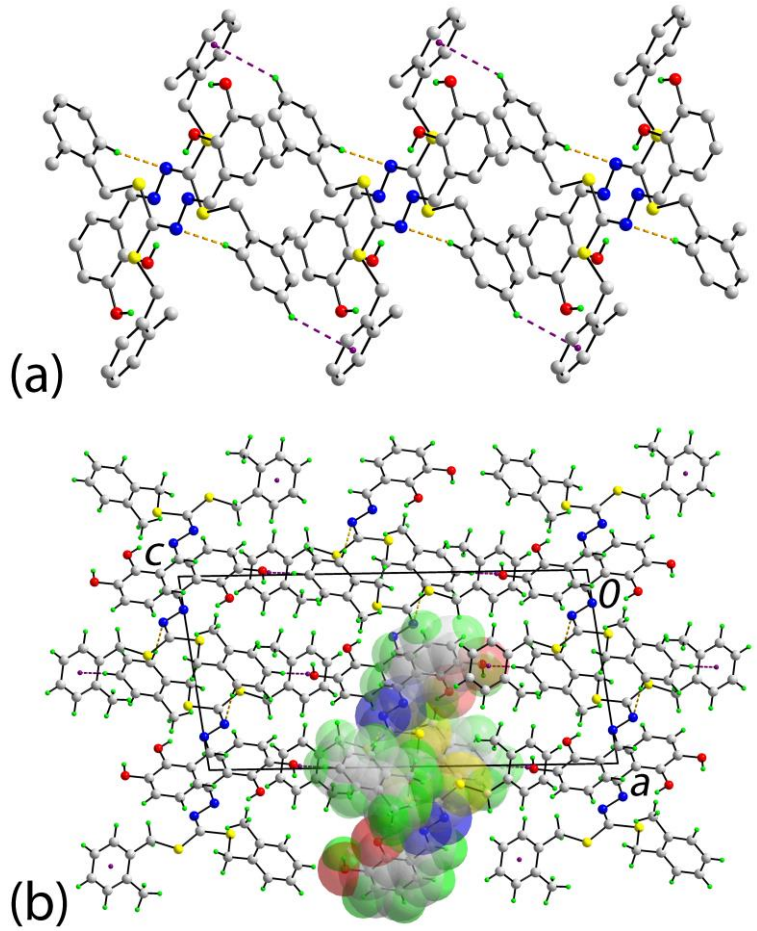

Fig. 2. Packing diagram for **1** with (a) a view of the supramolecular chain in the crystal, formed along the b-axis and sustained by tolyl-C–H…N(imine) and tolyl-C–H…π(tolyl) interactions between adjacent molecules shown as orange and purple dashed lines respectively. Non-acidic and non-participating H atoms are omitted. (b) a view of the unit cell along the b-axis. One supramolecular chain is highlighted in space-filling mode. (For interpretation of the references to colour in this figure legend, the reader is referred to the web version of this article.)

A structural analogue of **1** in which the m-OH group was replaced by a methoxy group showed through overlay of the two molecules (not shown), a great similarity in the molecular conformations, apart for the orientation of one of the o-tolyl groups which was folded towards the rest of the molecule as opposed to what was observed in **1** [40].

The gas phase B3LYP/6-311G(d,p) optimised structure of **1** is shown in Fig. 3. The calculated bond lengths and angles are in agreement with the values obtained from the crystallographic analysis above (see Table 2). This similarity was consistent with the absence of strong directional intermolecular interactions in the crystal. The deviations in the selected

bond lengths/angles of **1** ranged from 0.006-0.038 Å/0-3.3°, whereby the maximum bond length deviation corresponded to the C2–S1 bond and the maximum bond angle deviation corresponded to the N2–N1–C1 angle.

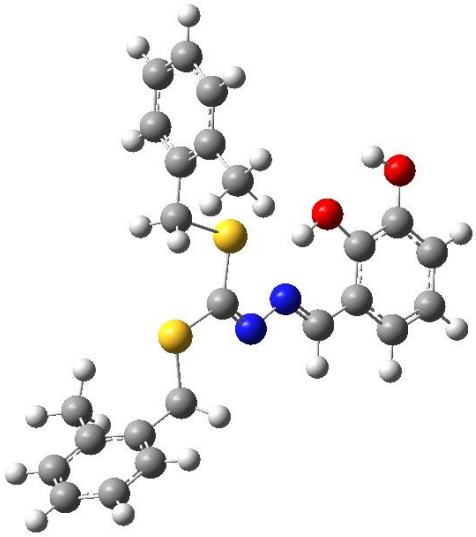

Fig. 3. B3LYP/6-311G(d,p) gas-phase geometry of **1**

Table 2

Selected molecular structure parameters of **1**

Bond length (Å)	Experimental	B3LYP/6-311G(d,p)
C2–S1	1.818(3)	1.856
S1–C1	1.739(2)	1.771
C1–S2	1.763(2)	1.787
S2–C10	1.828(3)	1.859
C1–N1	1.293(3)	1.287
N1–N2	1.407(2)	1.383
N2–C18	1.281(3)	1.291
Bond Angle (°)	Experimental	B3LYP/6-311G(d,p)
C1–S1–C2	102.0(1)	101.4
C1–S2–C10	103.0(1)	104.1
N2–N1–C1	111.5(2)	114.8
N1–N2–C18	113.3(2)	114.1
S1–C1–S2	117.5(1)	118.3

S1–C1–N1	120.1(2)	119.3
S2–C1–N1	122.4(2)	122.4

The X-ray and B3LYP/6-311G(d,p) C1–S1 and C1–S2 bond distances both indicated single bond character, consistent with a previous report [40]. The bond lengths of N1–N2 and C18–N2 were consistent with single and double bonds, respectively; the latter with an E-configuration. Despite the planarity in the central residue, there was little evidence for extensive delocalization of π-electron density over these atoms [41]; ~~The C1–N1, N1–N2 and C18–N2 bond lengths suggested limited conjugation over these atoms and the configuration about the N–N=C bond was *E* [40]~~. The S1-C1-S2 bond angle was systematically narrower than the S1–C1–N1 and S2–C1–N1 bond angles, again consistent with the single bond character of the C1–S1 and C1–S2 bonds.

*3.2. Hirshfeld surface analysis of **1***

The calculated Hirshfeld surfaces [42,43] for **1** were performed in accord with earlier studies on organic molecules [44] and provide additional insight into the supramolecular associations in the crystal of **1**. The intermolecular C–H...N interactions involving tolyl-C18 as the donor and imine-N2 as an acceptor leading to dimeric aggregation in the crystal are viewed as bright-red spots near these atoms on the Hirshfeld surface mapped over d_{norm} in Fig. 4a. The edge-to-edge short interatomic C...C contact involving dihydroxyphenyl-C24 is also viewed in Fig. 4a as a faint-red spot. The influence of the tolyl-C14–H...π(tolyl) interaction is evident from the Hirshfeld surface mapped over the electrostatic potential as blue and light-red regions corresponding to the donor and acceptor, respectively, in Fig. 4b. Referring to Table 3, the short interatomic C...H/H...C contacts involving tolyl-H14 in the crystal are highlighted in the Hirshfeld surface mapped with the shape-index property about a reference molecule in Fig. 4c.

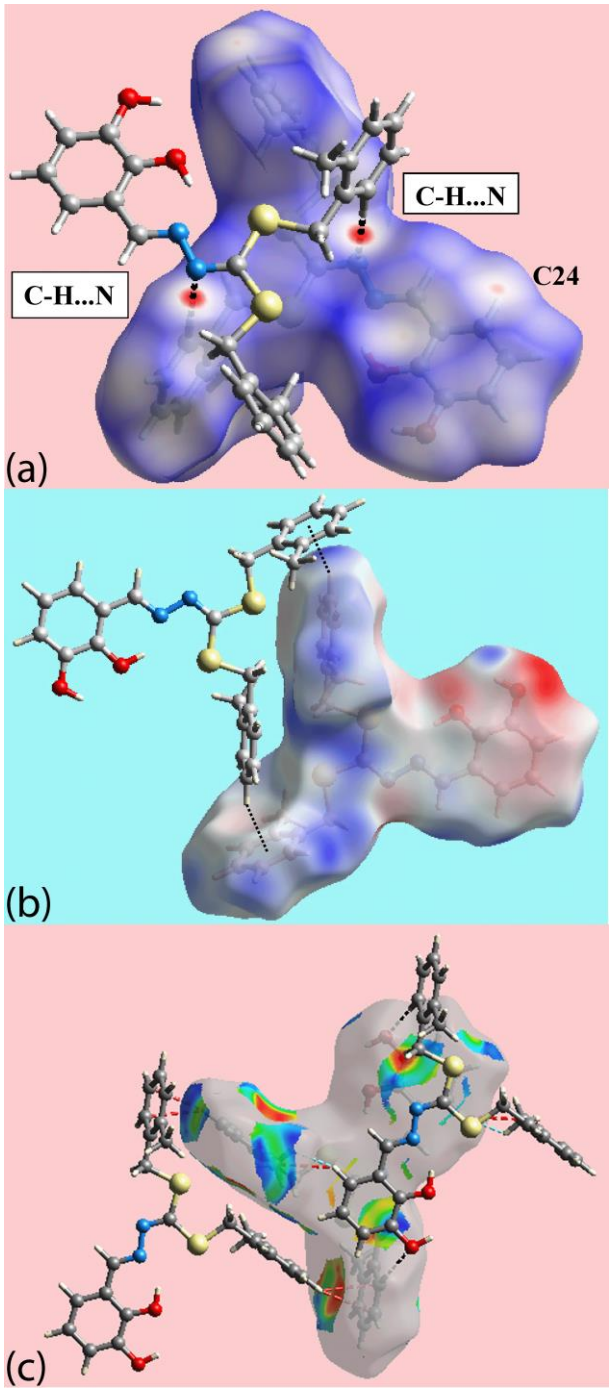

Fig. 4. Hirshfeld surfaces for **1**: (a) mapped over d_{norm} in the range -0.133 to +1.351 au and highlighting C–H...N interactions through black dotted lines, (b) mapped over the electrostatic potential in the range -0.060 to +0.037 au highlighting intermolecular C–H...π/π...H–C interactions as black dotted lines and (c) mapped with the shape-index property about a reference molecule highlighting short interatomic H...H, O...H/H...O and C...H/H...C contacts by sky-blue, black and red dashed lines, respectively. (For interpretation of the

references to colour in this figure legend, the reader is referred to the web version of this article.)

Table 3

Summary of short interatomic contacts in the molecular packing of **1**.

Contact	Distance (Å)	Symmetry operation
H17C...H24	2.17	1-x, -y, -z
C24...C24	3.354(4)	2-x, 2-y, -z
C7...H14	2.77	1-x, -y, -z
C8...H14	2.79	1-x, -y, -z
C13...H5	2.75	½+x, ½-y, ½-z
C20...H17B	2.75	x, 1+y, z
O1...H6	2.67	½+x, ½-y, ½+z
O2...H8	2.64	2-x, 1-y, -z
S1...C13	3.492(3)	1-x, -y, -z

The overall two-dimensional fingerprint plot for **1** characterising features of interatomic H...H, N...H/H...N and C...H/H...C contacts is illustrated in Fig. 5a. The percentage contributions from the different interatomic contacts to the Hirshfeld surface are summarised in Table 4. A pair of short spikes at $d_e + d_i \sim 2.2$ Å in the middle and at $d_e + d_i \sim 2.6$ Å flanking these peaks in Fig. 5a indicate the presence of short interatomic H...H contacts (Table 3) and the intermolecular C–H...N interactions (Table 1), respectively. The features due to interatomic C...H/H...C and O...H/H...O contacts shown in the overall fingerprint plot are viewed more clearly from those delineated into C...H/H...C and O...H/H...O contacts [45] in Figs 4b,c, respectively. The short interatomic C...H/H...C and O...H/H...O contacts summarized in Table 3 are viewed as the distribution of points in pairs at around $d_e + d_i <$ sum of their van der Waal radii, i.e. 2.72 Å and 2.90 Å in Figs 4b and c, respectively. The

small contribution of 2.0% from C...C and C...S/S...C contacts to the Hirshfeld surface are due to the presence of their respective short interatomic contacts (Table 3). The other interatomic contacts summarised in Table 4 are separated by relatively long distances and have a negligible effect upon the packing.

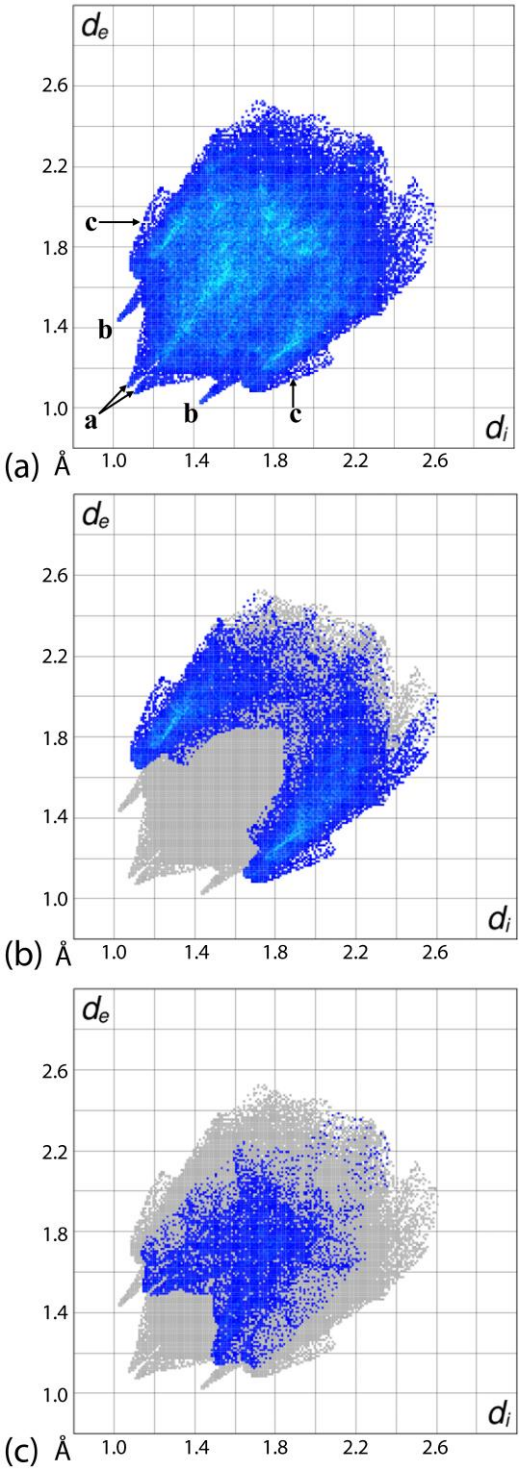

Fig. 5. (a) The overall two-dimensional fingerprint plot for **1** with labels a, b, c highlighting H...H, N...H/H...N and C...H/H...C contacts, respectively, (b) fingerprint plot delineated into C...H/H...C contacts and (c) fingerprint plot delineated into O...H/H...O contacts.

Table 4

Percentage contribution of intermolecular contacts to the Hirshfeld surface of **1**.

Contact	Percentage contribution
H…H	52.8
C…H/H…C	24.1
O...H/H...O	8.3
S...H/H...S	4.8
N...H/H...N	3.4
C...C	2.0
C...S/S...C	2.0
C...N/N...C	2.0
C...O/O...C	0.5
S...S	0.1

*3.3. Experimental and calculated vibrational spectra of **1***

The experimental and the calculated frequencies in the infrared spectra of **1** were in the range of 4000 to 280 cm^{-1} and 4000 to 0 cm^{-1}, respectively. The important infrared vibrations are summarised in Table 5. In order to minimize theoretical error, simulated vibrations were scaled by using a scaling factor of 0.9682 [46]. From the infrared spectrum, **1** did not show any medium bands at 3100 cm^{-1} due to *ν*(N-H) vibrations, providing strong evidence for the presence of the SC(-S)=N band. The stretching vibration modes of S-C-S for the experimental and calculated spectra were at 978 and 941 cm^{-1} respectively. The corresponding experimental and calculated vibration frequencies of *ν*(*o*-OH) appeared at

3497 and 3207 cm^{-1}, while *v*(*m*-OH) was observed at 3542 and 3654 cm^{-1}, respectively. The azomethine *v*(C=N) vibration frequencies for the experimental and calculated spectra were at 1678 and 1641 cm^{-1}, respectively. The differences in the vibrational frequencies can be explained by the fact that the experimental spectrum was obtained in the solid-state, while DFT calculations were run in the gas-phase.

Table 5

Experimental and DFT calculated vibrational frequencies for **1**

	Experimental	B3LYP/6-311G(d,p)
v(S–C–S)	978	941
v(C=N)	1678	1641
v(*o*-OH)	3497	3207
v(*m*-OH)	3542	3645

*3.4. NMR spectra of **1***

Selected experimental and simulated ^{1}H and ^{13}C NMR data are tabulated in Table 6. Experimentally, in the ^{1}H NMR spectrum, the absence of a resonance peak for NH (~13.00-14.00 ppm) was evidence that (**1**) was formed. This was in good agreement with the IR data which showed the absence of an *v*(NH) band at ca 3100 cm^{-1}. The upfield signals at 2.41 and 2.46 ppm suggested the presence of sp^3-type CH_3 protons and two clear signals at 4.31 and 4.51 ppm correspond to the CH_2 protons. The corresponding simulated chemical shifts of the CH_3 and CH_2 protons were calculated at 2.48, 2.54 ppm and 4.22, 4.48 ppm respectively. The duplication of the proton signals was also indicative of the formation of **1**. In the ^{13}C NMR experimental spectrum, two signals at 19.21 and 19.34 ppm correspond to CH_3 of the o-tolyl groups, and two signals at 34.02 and 35.38 ppm correspond to CH_2. The simulated ^{13}C NMR data showed the presence of CH_3 and CH_2 at 19.81, 19.94 and 40.86, 45.12, respectively. The duplication of the signals is again consistent with the formulation of **1**. A downfield signal at 167.27 ppm indicated the presence of a quaternary carbon attached the sulphur atoms. Finally, the absence of a signal at ~190-200 ppm due to the C=S functionality also indicated that the product was not the expected Schiff base [41,47].

Table 6

Experimental and calculated ^{1}H and ^{13}C NMR chemical shifts (ppm) for **1**

	Experimental	B3LYP/6-311G(d,p)
^{1}H NMR		
-CH_3	2.41, 2.46	2.48, 2.54
-CH_2	4.31, 4.51	4.22, 4.48
-CH	8.29	8.58
^{13}C NMR		
S–C–S	167.27	177.64
-CH_3	19.21, 19.34	19.81, 19.94
-CH_2	34.02, 35.38	40.86, 45.12
-C=N	159.94	164.88

*3.5. Absorption studies and frontier molecular orbital analysis of **1***

The experimental UV-vis spectrum of **1** showed a prominent absorption peak at 328 nm, whereas the theoretical absorption peak was observed at 325 nm. The HOMO and LUMO of **1** are shown in Fig. 6. The highest oscillator strength corresponded to HOMO-LUMO electron transfer at 325 nm. Figure 6 showed that the HOMO was predominantly centrered on the diester and azomethine moieties. Conversely the LUMO was largely centered on the 2,3-dihydroxyphenyl ring and as well as the diester and azomethine moieties. Thus, the excitation observed at 325 nm was assigned to be n→π*, where nonbonding electrons of the azomethine nitrogen at the ground state were excited to the π* LUMO.

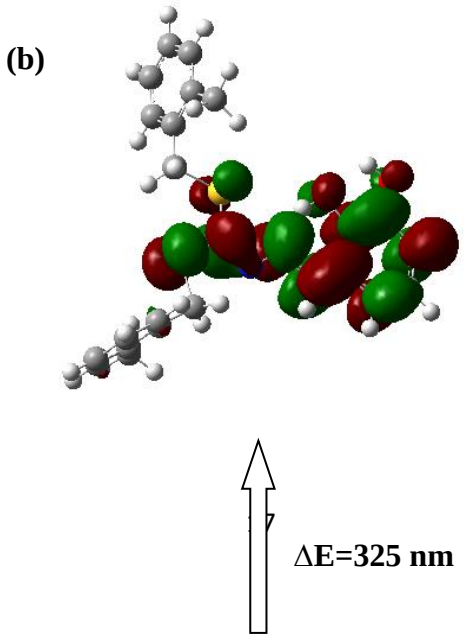

(a)

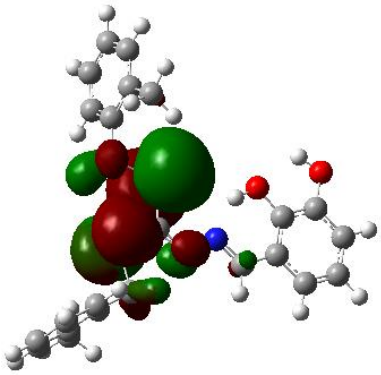

Fig. 6. Frontier molecular orbitals (a) HOMO and (b) LUMO of the optimised **1** using B3LYP/6-311G(d,p).

4. Conclusions

In this work, the unexpected formation of 3-[(1Z)-{2-[bis({[(2-methylphenyl) methyl]sulfanyl})methylidene]hydrazin-1-ylidene}methyl]benzene-1,2-diol **1** from the reaction between S-2-methylbenzyldithiocarbazate and 2,3-dihydroxybenzaldehyde is reported. The compound was fully characterised by FTIR, UV/Vis ^{1}H-NMR and ^{13}C-NMR spectroscopy and as well as single crystal X-ray diffraction analysis. The DFT approach using B3LYP/6-311G showed strong correlation with the experimental results: X-ray crystallography and spectroscopic data. Frontier molecular orbital analysis results showed the HOMO and LUMO localised on the diester and azomethine moieties, with additional localisation of the LUMO on the 2,3-dihydroxyphenyl ring, explaining the nature (n→π*) of the UV transition.

Acknowledgements

The authors gratefully acknowledge the Department of Chemistry, Universiti Putra Malaysia, for access to facilities. This research was funded by Universiti Putra Malaysia under the Geran Putra IPS (9504600) and the Malaysian Fundamental Research Grant Scheme (FRGS No. 01-01-16-1833FR). ENMY also wishes to acknowledge the MyPhD Malaysian Government Scholarship (MyBrain15) and the University of Newcastle Research Scholarship Central (UNRSC).

References

[1] M.A. Ali, S.E. Livingstone, Metal complexes of sulphur-nitrogen chelating agents, Coord. Chem. Rev. 13 (1974) 101–132.

[2] M.S. Begum, E. Zangrando, M.C. Sheikh, R. Miyatake, M.B.H. Howlader, M.N. Rahman, A. Ghosh, Bischelated complexes of a dithiocarbazate N,S Schiff base ligand: synthesis, characterization and antimicrobial activities, Transit. Met. Chem. 42 (2017) 553–563.

[3] M.L. Low, L. Maigre, M.I.M. Tahir, E.R.T. Tiekink, P. Dorlet, R. Guillot, T.B. Ravoof, R. Rosli, J.M. Pages, C. Policar, N. Delsuc, K.A. Crouse, New insight into the structural, electrochemical and biological aspects of macroacyclic Cu(II) complexes derived from S-substituted dithiocarbazate Schiff bases, Eur. J. Med. Chem. 120 (2016) 1–12.

[4] E.N.M. Yusof, T.B.S.A. Ravoof, J. Jamsari, E.R.T. Tiekink, A. Veerakumarasivam, K.A. Crouse, M.I.M. Tahir, H. Ahmad, Synthesis, characterization and biological studies of S-4-methylbenzyl-β-N-(2-furylmethylene)dithiocarbazate (S4MFuH) its Zn^{2+}, Cu^{2+}, Cd^{2+} and Ni^{2+} complexes, Inorganica Chim. Acta. 438 (2015) 85–93.

[5] F.R. Pavan, P.I. d. S. Maia, S.R.A. Leite, V.M. Deflon, A.A. Batista, D.N. Sato, S.G. Franzblau, C.Q.F. Leite, Thiosemicarbazones, semicarbazones, dithiocarbazates and hydrazide/hydrazones: Anti-Mycobacterium tuberculosis activity and cytotoxicity, Eur. J. Med. Chem. 45 (2010) 1898–1905.

[6] N. Awang, S.M. Mokhtar, N.M. Zain, N.F. Kamaludin, Evaluation of Antimicrobial Activities of Organotin (IV) Alkylphenyl Dithiocarbamate Compounds, Asian J. Appl. Sci. 8 (2015) 165–172.

[7] T.B.S.A. Ravoof, K.A. Crouse, M.I.M. Tahir, R. Rosli, D.J. Watkin, F.N.F. How, Synthesis, Characterisation and Biological Activities of 2-Methylbenzyl 2-(dipyridin-2-yl methylene)hydrazinecarbodithioate, J. Chem. Crystallogr. 41 (2011) 491–495.

[8] S. Shahzadi, S. Ali, M. Fettouhi, Synthesis, Spectroscopy, In Vitro Biological Activity and X-ray Structure of (4-Methylpiperidine-dithiocarbamato-S,S′)triphenyltin(IV), J. Chem. Crystallogr. 38 (2008) 273–278.

[9] M.T.H. Tarafder, M.A. Ali, D.J. Wee, K. Azahari, S. Silong, K.A. Crouse, Complexes of a tridentate ONS Schiff base. Synthesis and biological properties, Trans. Met. Chem. 25 (2000) 456–460.

[10] K.-B. Chew, M.T.. Tarafder, K.A. Crouse, A.. Ali, B.. Yamin, H.-K. Fun, Synthesis, characterization and bio-activity of metal complexes of bidentate N–S isomeric Schiff bases derived from S-methyldithiocarbazate (SMDTC) and the X-ray structure of the bis[S-methyl-β-N-(2-furyl-methylketone)dithiocarbazato]cadmium(II) complex, Polyhedron. 23 (2004) 1385–1392.

[11] M.T.H. Tarafder, K. Chew, K.A. Crouse, A.M. Ali, B.M. Yamin, H.K. Fun, Synthesis and characterization of Cu(II), Ni(II) and Zn (II) metal complexes of bidentate NS isomeric Schiff bases derived from S-methyldithiocarbazate (SMDTC): bioactivity of the bidentate NS isomeric Schiff bases , some of their Cu(II), Ni(II) and Zn(II) complexes and the X-ray structure of yhe bis[*S*-methyl-β-N-(2-furyl-methyl) methylenedithiocarbazato]zinc(II) complex, Polyhedron. 21 (2002) 2683–2690.

[12] H.P. Zhou, D.M. Li, P. Wang, L.H. Cheng, Y.H. Gao, Y.M. Zhu, J.Y. Wu, Y.P. Tian, X.T. Tao, M.H. Jiang, H.K. Fun, Synthesis, crystal structures, and two-photon absorption properties of dithiocarbazate Zn(II) and Pd(II) complexes, J. Mol. Struct. 826 (2007) 205–210.

[13] X. Wang, Z. Deng, B. Jin, Y. Tian, X. Lin, Study on the spectroelectrochemical properties of S -benzyl-N-(ferrocenyl-1-methyl-metylidene)-dithio-carbazate nickel(II) complex, Spectrochim. Acta Part A. 58 (2002) 3113–3120.

[14] H. Liu, L. Wu, F. Li, X. Wang, H. Pan, Y. Ni, J. Yang, S. Li, Y. Tian, J. Wu, Syntheses, characterizations and third-order NLO properties of a series of Ni(II), Cu(II) and Zn(II) complexes using a novel S-benzyldithiocarbazate ligand, Polyhedron. 121 (2017) 53–60.

[15] S.S.S. Raj, B.M. Yamin, Y.A. Yussof, M.T.H. Tarafder, H.K. Fun, K.A. Crouse, Trans-cis S-benzyl dithiocarbazate, Acta Crystallogr. Sect. C Cryst. Struct. Commun. C56 (2000) 1236–1237.

[16] M.A.A.A.A. Islam, M.C. Sheikh, M.S. Alam, E. Zangrando, M.A. Alam, M.T.H. Tarafder, R. Miyatake, Synthesis, characterization and bio-activity of a bidentate NS

Schiff base of S-allyldithiocarbazate and its divalent metal complexes: X-ray crystal structures of the free ligand and its nickel(II) complex, Transit. Met. Chem. 39 (2014) 141–149.

[17] T.-J. Khoo, M.K.B. Break, K.A. Crouse, M.I.M. Tahir, A.M. Ali, A.R. Cowley, D.J. Watkin, M.T.H. Tarafder, Synthesis, characterization and biological activity of two Schiff base ligands and their nickel(II), copper(II), zinc(II) and cadmium(II) complexes derived from S-4-picolyldithiocarbazate and X-ray crystal structure of cadmium(II) complex derived from pyridine-2-carboxaldehyde, Inorganica Chim. Acta. 413 (2014) 68–76.

[18] K.A. Crouse, K.B. Chew, M.T.H. Tarafder, A. Kasbollah, A.M. Ali, B.M. Yamin, H.K. Fun, Synthesis, characterization and bio-activity of S-2-picolyldithiocarbazate (S2PDTC), some of its Schiff bases and their Ni(II) complexes and X-ray structure of S-2-picolyl-β-N-(2-acetylpyrrole)dithiocarbazate, Polyhedron. 23 (2004) 161–168.

[19] T.B.S.A. Ravoof, K.A. Crouse, M.I.M. Tahir, F.N.F. How, R. Rosli, D.J. Watkins, Synthesis, characterization and biological activities of 3-methylbenzyl 2-(6-methyl pyridin-2-ylmethylene)hydrazine carbodithioate and its transition metal complexes, Transit. Met. Chem. 35 (2010) 871–876.

[20] S.A. Omar, T.B.S.A. Ravoof, M.I.M. Tahir, K.A. Crouse, Synthesis and characterization of mixed-ligand copper(II) saccharinate complexes containing tridentate NNS Schiff bases. X-ray crystallographic analysis of the free ligands and one complex, Transit. Met. Chem. 39 (2013) 119–126.

[21] F.N.-F. How, K.A. Crouse, M.I.M. Tahir, M.T.H. Tarafder, A.R. Cowley, Synthesis, characterization and biological studies of S-benzyl-β-N-(benzoyl) dithiocarbazate and its metal complexes, Polyhedron. 27 (2008) 3325–3329.

[22] H.-Q. Li, Y. Luo, D.-D. Li, H.-L. Zhu, (E)-4-Chlorobenzyl 3-(3-nitrobenzylidene) dithiocarbazate, Acta Crystallogr. Sect. E Struct. Reports Online. 65 (2009) o3101–o3101.

[23] Rigaku Oxford Diffraction. CrysAlis PRO. Agilent Technologies Inc., Santa Clara, CA, USA, 2015.

[24] G.M. Sheldrick, A short history of SHELX, Acta Crystallogr. Sect. A Found.

Crystallogr. A64 (2008) 112–122.

[25] G.M. Sheldrick, Crystal structure refinement with SHELXL, Acta Crystallogr. Sect. C Struct. Chem. C71 (2015) 3–8.

[26] L.J. Farrugia, WinGX and ORTEP for Windows: An update, J. Appl. Crystallogr. 45 (2012) 849–854.

[27] K. Brandenburg, DIAMOND, Crystal Impact GbR, (2006).

[28] C. Lee, W. Yang, R.G. Parr, Development of the Colle-Salvetti correlation-energy formula into a functional of the electron density, Phys. Rev. B. 37 (1988) 785–789.

[29] A.D. Becke, Density-functional thermochemistry. III. The role of exact exchange, J. Chem. Phys. 98 (1993) 5648–5652.

[30] K.-Y. Chen, H.-Y. Tsai, Synthesis, X-ray Structure, Spectroscopic Properties and DFT Studies of a Novel Schiff Base, Int. J. Mol. Sci. 15 (2014) 18706–18724.

[31] G. Scalmani, M.J. Frisch, B. Mennucci, J. Tomasi, R. Cammi, V. Barone, Geometries and properties of excited states in the gas phase and in solution: theory and application of a time-dependent density functional theory polarizable continuum model, J. Chem. Phys. 124 (2006) 94107.

[32] R. Ditchfield, Molecular Orbital Theory of Magnetic Shielding and Magnetic Susceptibility, J. Chem. Phys. 56 (1972) 5688–5691.

[33] K. Wolinski, J.F. Hinton, P. Pulay, Efficient Implementation of the Gauge-Independent Atomic Orbital Method for NMR Chemical Shift Calculations, J. Am. Chem. Soc. 112 (1990) 8251–8260.

[34] M.J. Frisch, G.W. Trucks, H.B. Schlegel, G.E. Scuseria, M.A. Robb, J.C. R., G. Scalmani, V. Barone, G.A. Petersson, H. Nakatsuji, X. Li, M. Caricato, A. Marenich, J. Bloino, B.G. Janesko, R. Gomperts, B. Mennucci, H.P. Hratchian, J. V. Ortiz, A.F. Izmaylov, J.L. Sonnenberg, D. Williams-Young, F. Ding, F. Lipparini, F. Egidi, J. Goings, B. Peng, A. Petrone, T. Henderson, D. Ranasinghe, V.G. Zakrzewski, J. Gao, N. Rega, G. Zheng, W. Liang, M. Hada, M. Ehara, K. Toyota, R. Fukuda, J. Hasegawa, M. Ishida, T. Nakajima, Y. Honda, O. Kitao, H. Nakai, T. Vreven, K. Throssell, J.A. Montgomery, Jr., J.E. Peralta, F. Ogliaro, M. Bearpark, J.J. Heyd, E.

Brothers, K.N. Kudin, V.N. Staroverov, T. Keith, R. Kobayashi, J. Normand, K. Raghavachari, A. Rendell, J.C. Burant, S.S. Iyengar, J. Tomasi, M. Cossi, J.M. Millam, M. Klene, C. Adamo, R. Cammi, J.W. Ochterski, R.L. Martin, K. Morokuma, O. Farkas, J.B. Foresman, D.J. Fox, Gaussian 09, Revision D.01, Wallingford CT. (2013).

[35] W. Rudorf, Reactions of Carbon Disulfide with C- nucleophiles, Sulfur Reports. 11 (1991) 51–141.

[36] M. Szczesio, A. Olczak, K. Gobis, H. Foks, M.L. Główka, Planarity of heteroaryldithiocarbazic acid derivatives showing tuberculostatic activity. IV. Diesters of benzoylcarbonohydrazonodithioic acid, Acta Crystallogr. Sect. C Cryst. Struct. Commun. C68 (2012) o99–o103.

[37] K. Gobis, H. Foks, E. Augustynowicz-Kopec, A. Napiorkowska, M. Szczesio, A. Olczak, M.L. Glowka, Synthesis, characterization, and tuberculostatic activity of novel 2-(4-nitrobenzoyl)hydrazinecarbodithioic acid derivatives, Monatshefte Fur Chemie. 143 (2012) 607–617.

[38] S. Tayamon, E.R.T. Tiekink, S.A. Omar, T.B.S.A. Ravoof, M.I.M. Tahir, K.A. Crouse, Crystal structure of a dithiocarbazate diester: E-bis(3-methylbenzyl)-1-(6-methylpyridin-2-yl)ethylidene-carbohydrazonodithioate, $C_{25}H_{27}N_3S_2$, Zeitschrift Fur Krist. - New Cryst. Struct. 229 (2014) 491–493.

[39] A.L. Spek, Structure validation in chemical crystallography, Acta Crystallogr. Sect. D Biol. Crystallogr. D65 (2009) 148–155.

[40] E.N.M. Yusof, T.B.S.A. Ravoof, M.I.M. Tahir, E.R.T. Tiekink, Crystal structure of 2-((1 E)-{2-[bis(2-methylbenzylsulfanyl)methylidene]hydrazin-1-ylidene}methyl)-6-methoxyphenol, Acta Crystallogr. Sect. E Crystallogr. Commun. E71 (2015) o242–o243.

[41] E.N.M. Yusof, T.B.S.A. Ravoof, E.R.T. Tiekink, A. Veerakumarasivam, K.A. Crouse, M.I.M. Tahir, H. Ahmad, Synthesis, characterization and biological evaluation of transition metal complexes derived from N, S bidentate ligands, Int. J. Mol. Sci. 16 (2015) 11034–11054.

[42] M.A. Spackman, P.G. Byrom, A novel definition of a molecule in a crystal, Chem.

Phys. Lett. 267 (1997) 215–220.

[43] M.J. Turner, J.J. McKinnon, S.K. Wolff, D.J. Grimwood, P.R. Spackman, D. Jayatilaka, M.A. Spackman, CrystalExplorer17, University of Western Australia, (2017).

[44] M.M. Jotani, J.L. Wardell, E.R.T. Tiekink, Crystal structure and Hirshfeld analysis of the kryptoracemate: Bis(mefloquinium) chloride p-fluorobenzenesulphonate, Zeitschrift Fur Krist. - Cryst. Mater. 231 (2016) 247–255.

[45] J.J. McKinnon, D. Jayatilaka, M.A. Spackman, Towards quantitative analysis of intermolecular interactions with Hirshfeld surfaces, Chem. Commun. 37 (2007) 3814–3816.

[46] P.M. Jeffrey, M. Damian, L. Radom, An Evaluation of Harmonic Vibrational Frequency Scale Factors, J. Phys. Chem. A. 111 (2007) 11683–11700.

[47] M.H.S.A. Hamid, A.N.A.H. Said, A.H. Mirza, M.R. Karim, M. Arifuzzaman, M. Akbar Ali, P. V. Bernhardt, Synthesis, structures and spectroscopic properties of some tin(IV) complexes of the 2-acetylpyrazine Schiff bases of S-methyl- and S-benzyldithiocarbazates, Inorganica Chim. Acta. 453 (2016) 742–750.